PERGAMON

Computers and Structures 72 (1999) 713–734

Computers & Structures

www.elsevier.com/locate/compstruc

Semielliptical-shaped sewer linings under installation conditions

S.M. Seraj[a], U.K. Roy[b], M.N. Pavlović[c,*]

[a]Department of Civil Engineering, Bangladesh University of Engineering and Technology, Dhaka, 1000 Bangladesh
[b]Department of Civil Engineering, University of Tokyo, Tokyo 113, Japan
[c]Department of Civil Engineering, Imperial College of Science, Technology and Medicine, London SW7 2BU, UK

Received 23 January 1997; accepted 19 November 1998

Abstract

This paper describes the results of a numerical parametric study on the structural response of closely packed semielliptical-shaped sewer linings. The effects of various restraint conditions which simulate different temporary support systems that may be used by the contractors during installation of the lining, and of different loading configurations which may arise at different stages of grouting the annulus gap between the lining and the sewer, have been thoroughly investigated. Comprehensive design curves, based on the allowable stress-limit, deflection-limit and (approximate) buckling criteria, are presented, covering the feasible range of geometric, material and loading parameters. © 1999 Elsevier Science Ltd. All rights reserved.

1. Introduction

Within the last few years a new discipline, expanding quickly and becoming a major consideration for designers of liquid storage and transmission facilities, has developed not only for those who work in the wastewater treatment field, but also for almost all engineers searching for better ways to control pollution. Lining is the name applied to this new technology. Lining, in a general sense, means any material laid down in a holding or conveyance facility to prevent the movement of liquid from one point where its presence is desirable or least objectionable to another point where its presence is undesirable. While liquid encompasses water, oil, brines, sewage, and chemical solutions of all types, the present research concentrates on sewage as the liquid. The definition of a holding facility can be taken to include such structures as concrete, steel or wooden tanks, in addition to cut-and-fill reservoirs, but it is the conveyance system of sewers, through which sewage is transmitted, that is being addressed in the present study. Apart from arresting the contamination of soil surrounding the sewers, lining technology can also be adopted in rehabilitating the existing old sewers, instead of replacing them, thus avoiding the traditional method of replacement of existing old sewers, which involves large capital expenditure and causes heavy disruption to traffic during the installation of the new sewers. Various shapes of sewer available in different countries are shown in Fig. 1. In the past, the structural responses of circular-, egg-, inverted egg- and horseshoe-shaped sewer linings under different installation and operational conditions have been investigated [1–7]. The present study concentrates on the behaviour of semielliptical-shaped sewer linings.

* Corresponding author. Fax: +44-171-594-5989.
E-mail address: m.pavlovic@ic.ac.uk (M.N. Pavlović)

PII: S0045-7949(98)00289-2

Nomenclature

A	dimensionless constants for maximum bending stress (staged grouting)
B_x, B_y	dimensionless constants for maximum deflection (staged grouting)
C	dimensionless constants for maximum bending stress (flotation)
D	diameter of circular lining
D_x, D_y	dimensionless constants for maximum deflection (flotation)
E	dimensionless constants for maximum bending stress (uniform pressure)
E_s	short-term modulus of elasticity of lining material
EF	enhancement factor for allowable grouting pressure
F_{cr}	critical axial force in circular lining
F_x, F_y	dimensionless constants for maximum deflection (uniform pressure)
G	unit (specific) weight of grout mix
H	excess head of grout (measured form crown of lining) corresponding to uniform pressure load
h	height of lining
K	$(G_w/E_s)(w/t)^3$
M	membrane stress at any point in lining
M_{cr}	critical buckling stress due to membrane action
M_t	total membrane stress
M_x	$D_x+F_x(H/w)$
M_y	$D_y+F_y(H/w)$
N_x	$D_x+F_x(p/Gw-h/w)$
N_y	$D_y+F_y(p/Gw-h/w)$
p	allowable grouting pressure measured at invert of lining
R	$(S_s/Gw)(t/w)^2$
RF	reduction factor for minimum permissible lining thickness
Q	$(360/\theta)^2-1$
S_s	allowable short-term bending stress of lining material
S_F	stiffness of lining, $(1/12)(E_s/(1-\nu^2))(t/w)^3$
S_t	total bending stress of lining material due to combined flotation and external pressure
t	thickness of lining
w	width of lining
α	dimensionless constants for maximum membrane stress (flotation)
β	dimensionless constants for maximum membrane stress (uniform pressure)
δ	deflection of lining
δ_t	total deflection of lining material due to combined flotation and external pressure
θ	angle between supports of arch
ν	Poisson's ratio

The linings are usually made of glass-reinforced plastic (GRP) or glass-reinforced cement (GRC). Steel linings are also used. A semielliptical-shaped lining (see Fig. 2) is to be inserted into the similarly shaped sewer after allowing for an annulus gap so that the sewer lining fits within the existing sewer with a roughly uniform gap between the lining and the sewer walls. The gap between the lining and the sewer is then filled with a cementitious grout which, when set, creates a composite sewer-lining structure.

During installation, the lining is subjected to grout pressure. In some cases, this may lead to overstressing of the lining at different sections due to excessive bending moment, which may cause failure of the lining pipe. Again, excessive deformation of any part of the lining might occur, affecting the serviceability of the relined sewer. Failure may also take place in the form of buckling due to excessive compressive forces. Thus, a properly designed sewer must comply to (bending) stress-limit, deflection-limit and buckling criteria. Here, the stress-limit criteria are so defined that the maximum bending stress developed during grouting must not exceed the allowable bending stress of the lining material. For the deflection-limit criteria, a maximum allowable deflection in the lining must not exceed 3% of the width of the lining (as advocated by the Water Research Centre in its Sewerage Rehabilitation Manual [8]). As regards the buckling criteria, the lining must be so designed that failure is not triggered by buckling owing to large hoop compression.

2. Grouting methods

In the course of installing sewer linings, staged or partial grouting and full grouting techniques are generally adopted. Staged or partial grouting is performed in two stages. The first stage involves grouting the annulus up to a predefined height of the lining, and this is followed by a second stage carried out after the grout of stage one has set. On the other hand, full grouting is performed in a single stage. This technique is more practical than staged grouting. However, during full grouting, the lining is subjected to higher

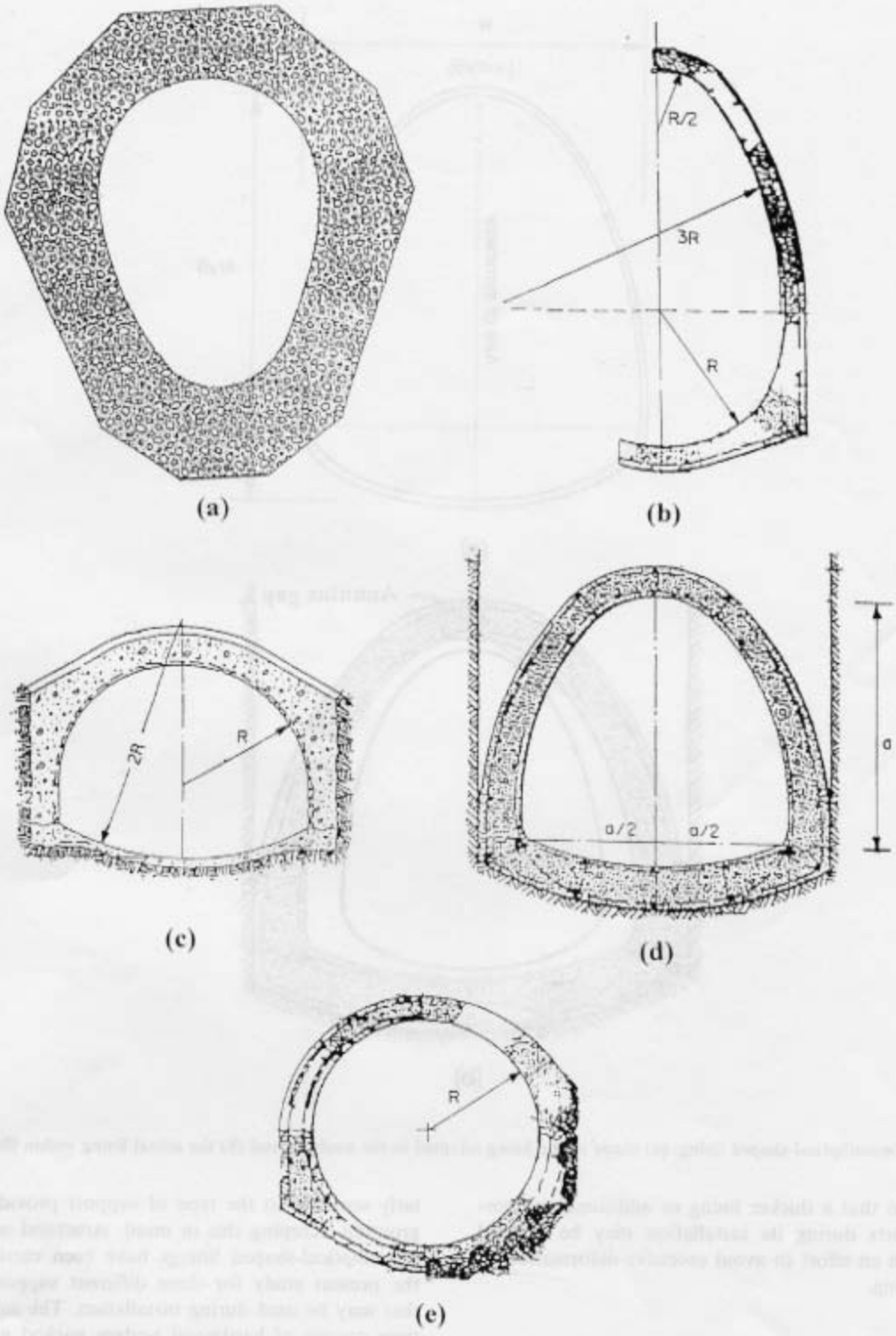

Fig. 1. Common shapes of sewer available in different countries: (a) egg-shaped (London, UK); (b) inverted egg-shaped (Louisville, USA); (c) horseshoe-shaped (Dallas, USA); (d) semielliptical-shaped (Tulsa, USA) and (e) circular-shaped (Dhaka, Bangladesh).

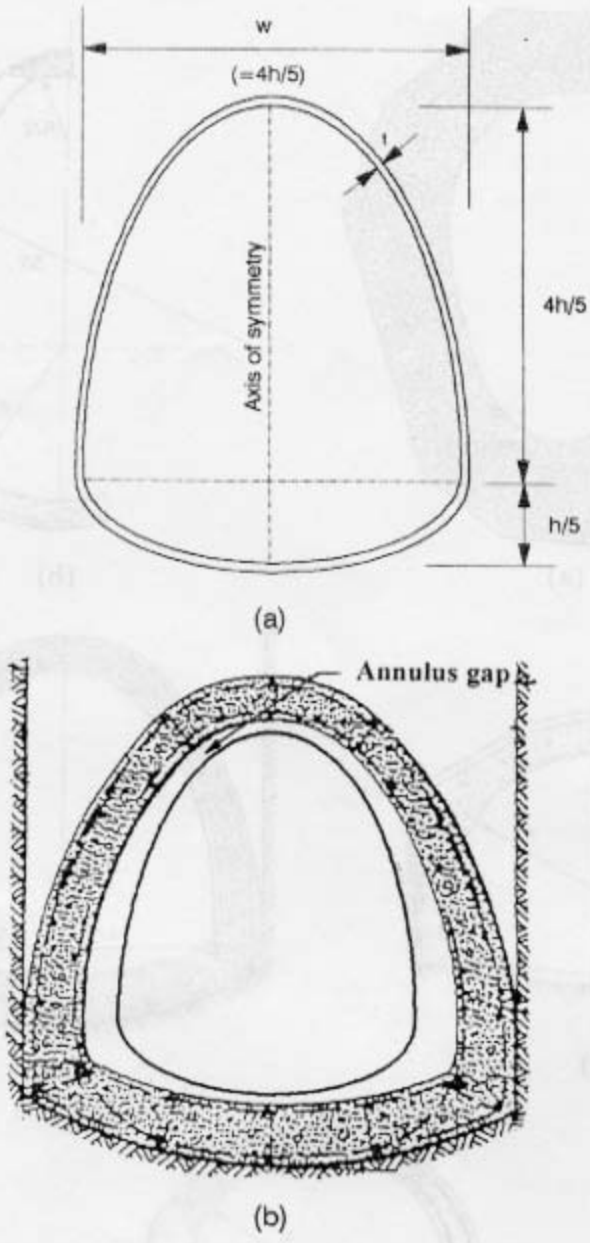

Fig. 2. Semielliptical-shaped lining: (a) shape of the lining adopted in the analysis, and (b) the actual lining within the sewer.

pressure so that a thicker lining or additional temporary supports during its installation may be deemed essential in an effort to avoid excessive deformation or overstressing.

3. Restraint conditions

The performance of various sewer linings is particularly sensitive to the type of support provided during grouting. Keeping this in mind, structural analyses of semielliptical-shaped linings have been carried out in the present study for three different support systems that may be used during installation. The support systems consist of hardwood wedges packed at different locations around the cross-section of the lining on the outside, together with internal struts positioned at the same locations. It is assumed that the packing between

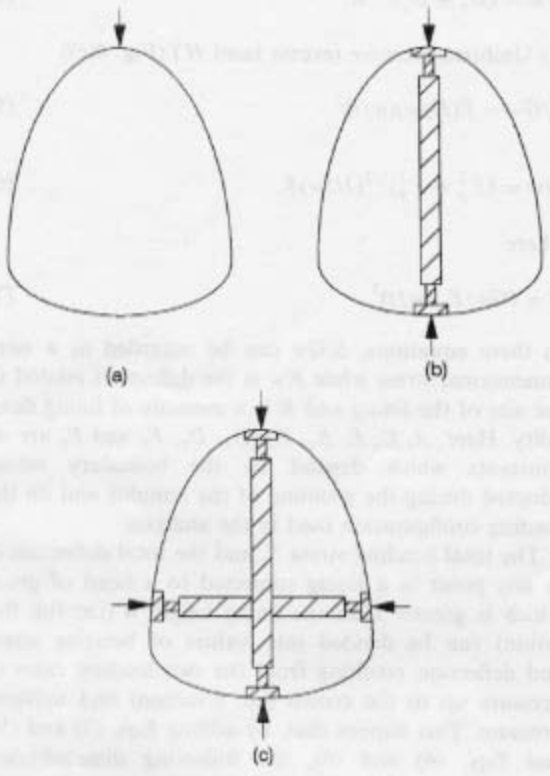

Fig. 3. Semielliptical-shaped lining: the support systems studied (a) boundary condition 1, (b) boundary condition 2, and (c) boundary condition 3.

the sewer and the lining is closely spaced (typically, with spacing not exceeding the width of the lining), so that the structure can be studied by means of a two-dimensional finite-element (FE) model. The three possible support systems considered in the present study are shown in Fig. 3.

Boundary condition 1 consists solely of a restraint at the crown (top) of the lining—usually achieved by inserting a wooden block between lining and sewer so as to preserve the annular gap at that location—as shown in Fig. 3(a). It is to be noted here that grout is usually injected through the invert (bottom) of the lining. As the grout moves forward and upward during its injection, this may push the lining upwards and thereby reduce the annulus gap between the sewer and the lining. This is why a restraint at the crown is always expected. The second support system, shown in Fig. 3(b) as boundary condition 2, comprises restraints at both the crown and the invert of the lining. Like boundary condition 1, boundary condition 2 imposes restraints on the vertical movement of sewer linings, but now at the invert as well as the crown. Consequently, this boundary condition is vertically stiffer than the former. Boundary Condition 3 consists of restraints at the crown, invert and at one-third height from the invert of the linings (Fig. 3(c)). In addition to vertical restraints, it restricts the horizontal movement of the lining at the one-third height of the lining. (Unlike other lining types, horizontal restraints at the springings (at one-fifth height in the present case) have been found to be ineffective, such restraints being too close to the invert [9].)

4. Loading configurations

Three loading configurations, namely staged-grouting pressure, flotation pressure and uniform pressure are included throughout the analysis unless otherwise specified. Here, staged-grouting pressure corresponds to pressure from grout surrounding the lining up to the one-third height of the lining, as shown in Fig. 4(a), and so simulates the first phase of staged grouting. Flotation pressure involves a head of grout up to the crown, as in Fig. 4(b). In this situation, the lining is just covered by grout and hence the buoyancy force acting on the lining is the maximum that can occur.

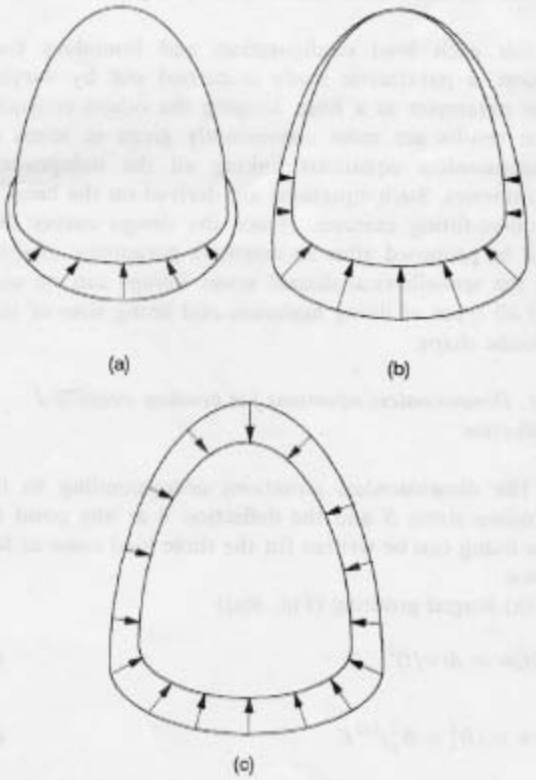

Fig. 4. Semielliptical-shaped lining: the loading configurations studied (a) staged grouting, (b) flotation pressure, and (c) uniform pressure.

The uniform-pressure case, shown in Fig. 4(c), corresponds to the uniform pressure which is applied on the lining as a consequence of an excess head of grout. Clearly, flotation pressure and uniform pressure can be superimposed in order to simulate any grout pressure applied on the lining during full grouting.

5. Load calculations

In the case of the loading corresponding to flotation and to the first phase of staged grouting, the applied load is defined by the lining height h and the specific weight of grout mix G. In these two loading cases, the applied pressure at any point on the lining can be calculated by multiplying the specific weight of the grout mix by the distance from the top of the grouting to the point at which the pressure is calculated. For the uniform-load case, on the other hand, the external load is defined by the values of excess head of grout H (and its specific weight G) and is independent of the height of the lining.

6. Mathematical formulation of the analysis

For each load configuration and boundary condition, a parametric study is carried out by varying one parameter at a time, keeping the others constant. The results are most conveniently given in terms of dimensionless equations linking all the independent parameters. Such equations are derived on the basis of a curve-fitting exercise. Hence the design curves that will be proposed after an extensive parametric analysis of the semielliptical-shaped sewer linings can be used for all types of lining materials and lining sizes of that specific shape.

6.1. Dimensionless equations for bending stress and deflection

The dimensionless equations corresponding to the bending stress S and the deflection δ at any point on the lining can be written for the three load cases as follows:

(a) Staged grouting (Fig. 4(a))

$$S/Gw = A(w/t)^2 \tag{1}$$

$$\delta/w = (B_x^2 + B_y^2)^{1/2} K \tag{2}$$

(b) Flotation (or pressure up to the level of crown) (Fig. 4(b))

$$S/Gw = C(w/t)^2 \tag{3}$$

$$\delta/w = (D_x^2 + D_y^2)^{1/2} K \tag{4}$$

(c) Uniform pressure (excess head H) (Fig. 4(c))

$$S/Gw = E(H/w)(w/t)^2 \tag{5}$$

$$\delta/w = (F_x^2 + F_y^2)^{1/2} (H/w) K \tag{6}$$

where

$$K = (Gw/E_s)(w/t)^3 \tag{7}$$

In these equations, S/Gw can be regarded as a non-dimensional stress while δ/w is the deflection related to the size of the lining and K is a measure of lining flexibility. Here, A, C, E, B_x, B_y, D_x, D_y, F_x and F_y are all constants which depend on the boundary set-up adopted during the grouting of the annulus and on the loading configuration used in the analysis.

The total bending stress S_t and the total deflection δ_t at any point in a lining subjected to a head of grout which is greater than the lining height h (i.e. full flotation) can be divided into values of bending stress and deflection resulting from the two loading cases of pressure up to the crown (i.e. flotation) and uniform pressure. This implies that, by adding Eqs. (3) and (5), and Eqs. (4) and (6), the following dimensionless equations for the total bending stress and the total deflection, respectively, can be written as

$$S_t/Gw = \left|(C + E(H/w))(w/t)^2\right| \tag{8}$$

$$\delta_t/w = (M_x^2 + M_y^2)^{1/2} K \tag{9}$$

where

$$M_x = D_x + F_x(H/w) \tag{10a}$$

$$M_y = D_y + F_y(H/w) \tag{10b}$$

Since, as mentioned earlier, the maximum bending stress and the maximum deflection in a lining must not exceed the respective values of S_s and $0.03\ w$, the values of S_t and δ_t in Eqs. (8) and (9) can be replaced by S_s and $0.03\ w$, respectively. As the point of injection of the grout is usually located at the invert of the lining, it is convenient to replace the value of H in Eqs. (8) and (9) by the equivalent expression $(p/G-h)$, where p is the allowable grouting pressure measured at the invert of the lining. As a result, Eqs. (8) and (9) can be rewritten to produce the following design equations

$$R = \left|C + E(p/Gw - h/w)\right| \tag{11}$$

where

$$R = (S_s/Gw)(t/w)^2 \tag{12}$$

and

$$0.03/K = (N_x^2 + N_y^2)^{1/2} \tag{13}$$

where

$$N_x = D_x + F_x(p/Gw - h/w) \tag{14a}$$

$$N_y = D_y + F_y(p/Gw - h/w) \tag{14b}$$

6.2. Dimensionless equations for membrane stress

Although buckling is unlikely to be the governing criterion in semielliptical-shaped linings if adequate temporary restraints are provided during their installation, the fact that axial forces in these linings are of comparable magnitudes compared with those in circular ones suggests that buckling considerations should not be neglected altogether. In order to consider buckling, albeit approximately, in the analysis, the simplified approach in Ref. [5] for circular linings has been followed. During the course of this investigation it has been observed that the dimensionless Eqs. (15) and (16) below, which had been found suitable for circular linings [5] under flotation and uniform pressure cases, respectively, are also reasonably applicable to semielliptical-shaped linings once w is inserted instead of D. Here, M corresponds to the membrane stress at any point in the lining.

1. Flotation

$$M/Gw = \alpha(w/t) \tag{15}$$

2. Uniform pressure

$$M/Gw = \beta(w/t)(H/w) \tag{16}$$

where α and β are constants which depend on the boundary condition selected during installation.

The total direct membrane stress (M_t) at any point in a lining subjected to a head of grout which is greater than the lining height h (i.e. full grouting), can be obtained by adding the values of membrane stresses resulting from each of the flotation loading and the uniform pressure. This leads to the following dimensionless equation for the total membrane stress in the lining:

$$(M_t/Gw)(t/w) = (\alpha + \beta(H/w)) \tag{17}$$

In Eq. (17), the replacement of the value of H by the equivalent expression $(p/G - h)$ and of h/w by 1.25, produces the following generic design equation for the different boundary conditions:

$$(M_t/Gw)(t/w) = \alpha + \beta(p/Gw - 1.25) \tag{18}$$

Here, the value of the critical grouting pressure, that can be applied on the lining during its installation, is based on a direct stress-limit criteria which is equal to the critical buckling stress due to membrane action M_{cr} in a hinged arch of equivalent radius and unrestrained length [8]. The value of M_{cr} is given by the following equation:

$$(M_{cr}/Gw)(t/w) = 4.0Q(S_F/Gw) \tag{19}$$

where S_F is the stiffness of the lining given by

$$S_F = (1/12)(E_s/(1 - \nu^2))(t/w)^3 \tag{20}$$

Q in Eq. (19) is a constant which depends on the angle θ between the hinges of the arch and is expressed as follows:

$$Q = (360/\theta)^2 - 1 \tag{21}$$

so that Q takes on the values 3 and 15 for boundary conditions 2 and 3, respectively.

By equating expressions (18) and (19) and using the appropriate value of Q from Eq. (21), a general design equation for the critical buckling pressure can be derived, albeit approximately, as follows:

$$4Q(S_F/Gw) = \alpha + \beta(p/Gw - 1.25) \tag{22}$$

The approximation implicit in this simplified buckling criterion is the adoption of hinges at the restrained points (thus neglecting continuity) [5] and in approximating the effective arc by an equivalent circular one.

6.3. Design criteria

For any particular lining geometry and material properties, the above equations must be satisfied at the locations of maximum bending stress, deflection and axial stress in the lining. The maximum allowable grouting pressure p which can be applied on the lining during grouting is the minimum of the p values as determined by all the criteria described in the previous two sections.

7. Two-dimensional finite-element model

A linear two-dimensional FE model is used in order to simulate the behaviour of semielliptical-shaped linings under various probable loads during installation. It can be seen from the shape of the semielliptical-shaped sewer of Fig. 2 that its bottom corners have sharp bends. Since higher concentrated stresses are

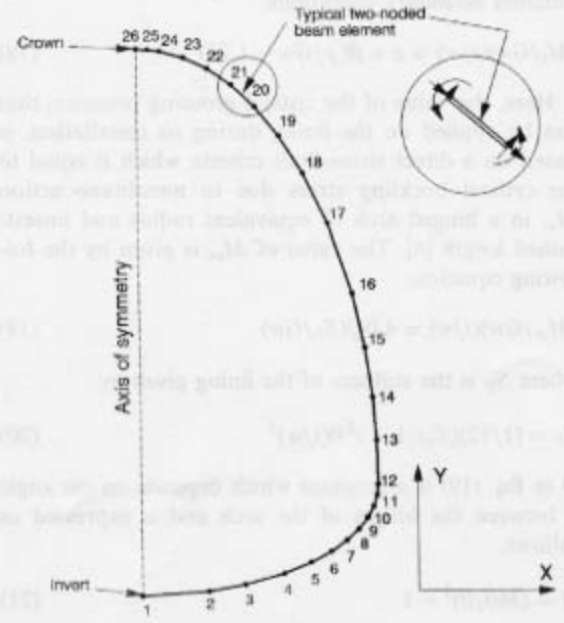

Fig. 5. Semielliptical-shaped lining: two-dimensional FE mesh adopted in the analysis.

expected at, or close to, these sharp bends, these stress concentrations may be catered for by increasing the lining thickness at the corners or by smoothening the corners. In the present study, the corners of the sewer lining have been given a slightly different geometry than that of the actual sewer. While the shape of the lining adopted for the analysis has been shown in Fig. 2(a), the actual lining geometry of the semielliptical-shaped sewer is given in Fig. 2(b). The shape of the lining consists of two half ellipses. The major axis of the horizontal ellipse equals the minor axis of the vertical (half-) ellipse (this common dimension being $4h/5$). The minor axes of both the ellipses are half of their respective major axes. This leads to smoothness (as well as continuity of both slope and curvature) at the sharp ends. It is clear that the height of the lining h is 1.25 times its width (i.e. $h/w = 1.25$); also, the annulus gap between the sewer and the lining becomes non-uniform, with a slightly higher gap near the bends.

In the analysis, the thickness of the lining is assumed to be constant all around the cross-section. Owing to symmetry of the lining geometry, the loading and the boundary conditions about the vertical axis (i.e. Y-axis), only half of the cross-section, shown in Fig. 5, is analysed. The elements used in the analysis are two-noded beam elements each having three degrees of freedom (horizontal and vertical displacement, and rotation) at each node. The mesh adopted consists of 25 elements, the node numbers corresponding to crown, one-third height and invert being 26, 14 and 1, respectively.

The restraints due to the support system shown in Fig. 3 are simulated numerically in the analysis by fixing the horizontal and vertical components of displacement at the corresponding nodal points. This involves a small approximation in that the deformation in the restraining struts is ignored, the strut being very stiff compared with the lining. As half of the cross-section is analysed, the horizontal and rotational components of displacements at nodes 1 and 26 of the lining are fully restrained. In addition, in Fig. 5, the vertical displacement at node 26 is set to zero for boundary condition 1 while the vertical displacements at both nodes 1 and 26 are made equal to zero for boundary condition 2. Similarly, restraints have been imposed on the vertical displacements at nodes 1 and 26, and on vertical and horizontal displacements at node 14 in order to simulate boundary condition 3.

The various loading configurations shown in Fig. 4 have been simulated by applying equivalent point loads at appropriate nodes.

8. Computation of constants

As already explained, for each load and boundary condition, the parametric analysis is carried out by varying one parameter at a time, keeping the others

Table 1
Dimensionless constants for the maximum bending stress in the lining. (*Note*: positive values of A, C and E imply tensile stresses in the inner surfaces of the lining)

	Coefficient	Boundary condition 1		Boundary condition 2		Boundary condition 3	
Staged grouting	A	0.362	Node 26	−0.1153	Node 1	0.0496	Node 1
Flotation	C	0.428	Node 26	0.1970	Node 26	−0.0970	Node 1
		−0.208	Node 9	−0.1020	Node 9	0.0520	Node 26
Uniform pressure	E	−0.400	Node 26	−0.303	Node 9	0.1100	Node 26
		−0.200	Node 9	−0.1590	Node 26	−0.0694	Node 1

Table 2
Dimensionless constants for the maximum deflections in the lining. (*Note*: inward deflections are taken as positive)

	Coefficient	Boundary condition 1		Boundary condition 2		Boundary condition 3	
Staged grouting	B_x	0.0000	Node 1	−0.00538	Node 17	0.00010	Node 4
	B_y	0.0681	Node 1	−0.00548	Node 17	0.00085	Node 4
Flotation	D_x	0.0000	Node 1	0.00785	Node 16	0.00019	Node 3
		−0.0240	Node 16			0.00128	Node 17
	D_y	0.0607	Node 1	0.00052	Node 16	0.00160	Node 3
		−0.0220	Node 16			0.00031	Node 17
Uniform pressure	F_x	0.0631	Node 16	0.03	Node 16	0.00210	Node 17
		0.0000	Node 1			0.00013	Node 3
	F_y	0.0450	Node 16	0.0233	Node 16	0.00055	Node 17
		−0.0634	Node 1			0.00110	Node 3

unchanged. The results (bending stresses, deflections and axial stresses) are given in terms of dimensionless equations linking all the independent parameters together as described earlier. The non-dimensional bending stress (S/Gw) and deflection (δ/w) are plotted against $(w/t)^2$ and lining flexibility K, respectively, for staged grouting and flotation load, and against $(H/w)(w/t)^2$ and $(H/w)K$ for uniform pressure. Similarly, the non-dimensional membrane stress (M/Gw) is plotted against (w/t) and $(w/t)(H/w)$, respectively for flotation and uniform-pressure cases. From these plots, dimensionless constants for the maximum bending stress, maximum deflection and maximum membrane stress in the lining are computed for different boundary conditions and different loading configurations. These are listed in Tables 1–3, respectively.

9. Full-grouting design curves

9.1. Stress-limit criteria

9.1.1. Boundary condition 1: restrained at crown only

The values of the bending-stress constants A, C and E for this boundary condition for different loading conditions are shown in Table 1. Of all the values of A, C and E for boundary condition 1 in Table 1, the value of C (in the case of flotation load) is the highest (0.428) and it occurs at node 26 of the lining. This means that the stress developed at node 26 (i.e. at the crown) of the lining as a result of the flotation load is the maximum of all the load cases taken into consideration in performing this analysis. The value of E for uniform load also has its maximum value (0.4) at node 26. The maximum values of C and E are, however, of opposite sense. Hence, when the full grouting load (flotation plus uniform pressure) is simulated, the stress developed at the crown has a value less than that developed due to flotation load alone. That is why the combined bending stress at all other nodes of the FE mesh were also computed. It has been found from this exercise that the maximum combined bending stress develops at node 9, and not at node 26. So, the values of C and E, as are computed at node 9, are also listed in Table 1. From the above discussion, it can be inferred that:

1. the value of R must be at least 0.428 to withstand the flotation load.
2. for full grouting load, the value of R at node 26 will be (from Eq. (11))

$$R = |0.428 - 0.400(p/Gw - 1.25)|$$
$$= |0.928 - 0.4p/Gw| \quad (23)$$

3. for full grouting load, the value of R at node 9 follows the relationship (from Eq. (11)

Table 3
Dimensionless constants for the maximum direct membrane stress in the lining

	Constant	Boundary condition 2		Boundary condition 3	
Flotation	α	0.512	Node 9	0.484	Node 9
				0.212	Node 21
Uniform pressure	β	0.730	Node 9	0.504	Node 21
				0.371	Node 9

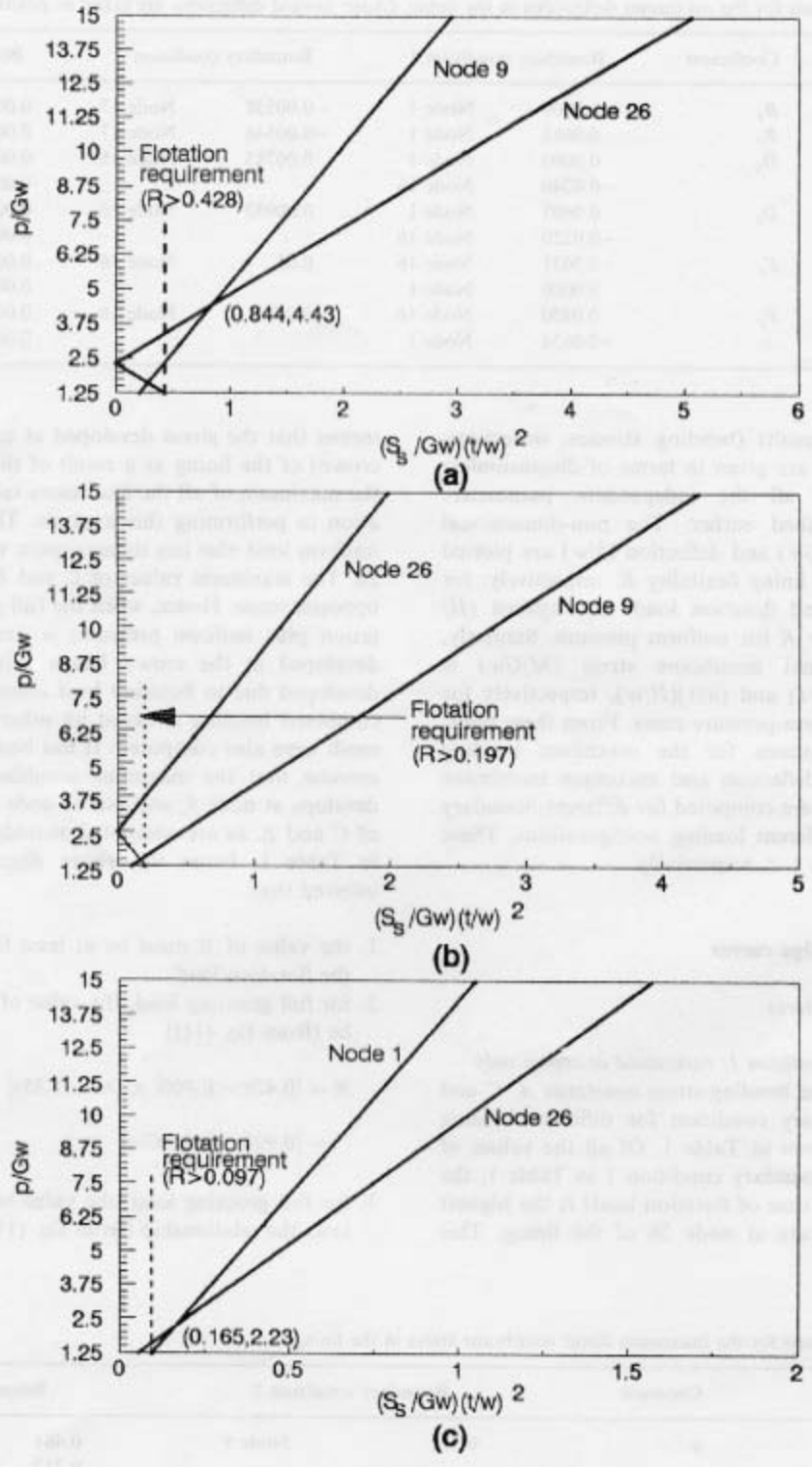

Fig. 6. Semielliptical-shaped lining: maximum bending stresses at nodes 9 and 26 of the lining for flotation and additional external pressure under (a) boundary condition 1, (b) under boundary condition 2, and (c) at nodes 1 and 26 under boundary condition 3.

$$R = |-0.208 + (-0.20)(p/Gw - 1.25)|$$
$$= |0.042 - 0.2p/Gw| \quad (24)$$

These equations are plotted in Fig. 6(a). The plot of the equation for node 9 cuts that for node 26, beyond the flotation limit, at the point (0.844,4.43). It is clear from Fig. 6(a) that the allowable grouting pressure resulting from Eq. 24 (at node 9) becomes dominant within the values of R ranging from 0.428 to 0.844 (i.e. p/Gw ranging from 2.35 to 4.43). Once the value of R exceeds 0.844, the bending stress at node 26 becomes critical. Staged grouting is not critical in comparison to the full grouting load. The relevant permissible pressures can readily be obtained, if required, by means of Eq. 1.

9.1.2. Boundary condition 2: restrained at crown and invert

In this boundary condition, it is seen that the maximum bending stresses for staged grouting, flotation and uniform pressures are located at nodes 1, 26, and 9 of the lining, respectively, the respective values of A, C and E are shown in Table 1.

The maximum bending stress developed at node 1, due to staged grouting, is less than that resulting from the flotation load for which case the maximum stress occurs at node 26. Again, the node at which the maximum stress develops due to uniform pressure (node 9) differs from that resulting from the flotation load (node 26). Hence, Eq. (11) must be satisfied at both the above nodes in the case of full (i.e. combined) grouting load. It is to be noted here that the combined bending stresses at all other nodes were calculated separately but were found to be less critical than those at nodes 9 and 26. All this leads to the following two design equations which are shown graphically in Fig. 6(b). At node 26,

$$R = |0.197 + (-0.159)(p/Gw - 1.25)|$$
$$= |0.396 - 0.159p/Gw| \quad (25)$$

and at node 9,

$$R = |-0.102 + (-0.303)(p/Gw - 1.25)|$$
$$= |0.277 - 0.303p/Gw| \quad (26)$$

Unlike the earlier boundary condition 1, for the present boundary condition the plot of Eq. (26) at node 9 does not intersect the plot of Eq. (25) at node 26 beyond the flotation requirement. It is apparent, therefore, that the stress at node 9 is always critical beyond the flotation requirement ($R > 0.197$), and this is clear from Fig. 6(b). As in boundary condition 1, staged grouting is not critical in this boundary condition, as can be seen from Table 1.

9.1.3. Boundary condition 3: restrained at crown, invert and one-third height from invert

Following a similar reasoning to that described for boundary conditions 1 and 2, in this case Eq. (11) must be satisfied at both the nodes 1 and 26. Once again, the maximum stress developed due to the flotation load is of opposite sense to that arising from the uniform pressure case. As before, the combined bending stresses at all other nodes were also computed, but the ensuing results proved to be less critical than those at nodes 1 and 26. Hence, the two design equations can be written as follows (using Eq. (11)). At node 1,

$$R = |-0.097 + (-0.0694)(p/Gw - 1.25)|$$
$$= |-0.01025 - 0.0694p/Gw| \quad (27)$$

and at node 26,

$$R = |0.0572 + (0.11)(p/Gw - 1.25)|$$
$$= |-0.0803 + 0.11p/Gw| \quad (28)$$

These two equations are plotted in Fig. 6(c). It is clear from the figure that the bending stress at node 1 is critical for the values of R within the range 0.097–0.165. Once R exceeds 0.165, the bending stress at node 26 determines the allowable grouting pressure based on stress-limit criteria.

9.1.4. Summary of stress-limit criteria

All the findings obtained for the three boundary conditions described earlier, are summarized in Fig. 7. Once a boundary condition is selected and the geometrical and material parameters are chosen, a value of allowable grouting pressure, based on stress-limit criteria, can be obtained from this figure.

It is seen from Fig. 7 that, for a given value of R, boundary condition 3 gives allowable grouting pressures much higher than those of boundary conditions 1 and 2. On the other hand, the adoption of boundary condition 2 instead of boundary condition 1 does not have a significant effect on the allowable grouting pressure.

9.2. Deflection-limit criteria

9.2.1. Boundary condition 1: restrained at crown only

Among the values of the constants B_X, B_Y, D_X, D_Y, F_X and F_Y tabulated in Table 2 for different loadings (staged grouting, flotation and uniform pressure respectively) under boundary condition 1, the constant $\sqrt{(B_X^2 + B_Y^2)}$ has the highest value. This means that the

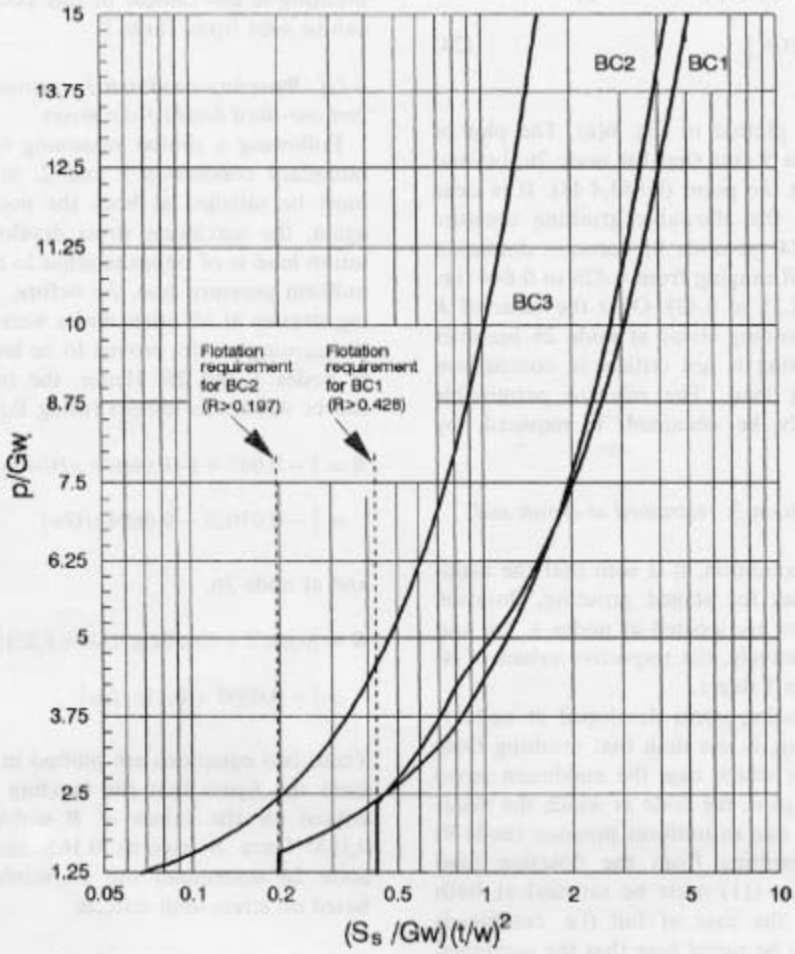

Fig. 7. Semielliptical-shaped lining: allowable grouting pressure, based on stress-limit criteria, for various boundary conditions.

maximum deflection resulting from staged grouting is greater than any deflections arising from other loadings if these were applied on the lining individually. This leads to the requirement that a minimum value of $0.03/K$ equal to 0.0681 is needed in order for the lining to withstand the maximum allowable deflection (3% of w) as recommended by the Water Research Centre (WRC) [8].

In the case of flotation, the maximum displacement occurred at node 1, whereas that for the uniform-pressure case occurred at node 16. This suggests that Eq. (13) must be satisfied at both nodes 1 and 16, which leads to the following two design equations at these nodes: At node 1,

$$\frac{0.03}{K} = |0.14 - 0.0634p/Gw| \tag{29}$$

and at node 16,

$$\frac{0.03}{K} = |0.0775p/Gw - 0.129| \tag{30}$$

These two equations are plotted in Fig. 8(a). It is seen from the figure that the displacement at node 16 is always critical and determines the allowable grouting pressure on the lining under combined flotation and uniform-pressure loading ($p/Gw > 2.543$) that exceeds the partial-grouting requirement.

9.2.2. *Boundary condition 2: restrained at crown and invert*

The maximum deflection in the lining resulting from the combined effect of flotation and uniform pressure is located at node 16 of the lining. This implies that Eq. (13) must be satisfied at node 16 for values of p/G

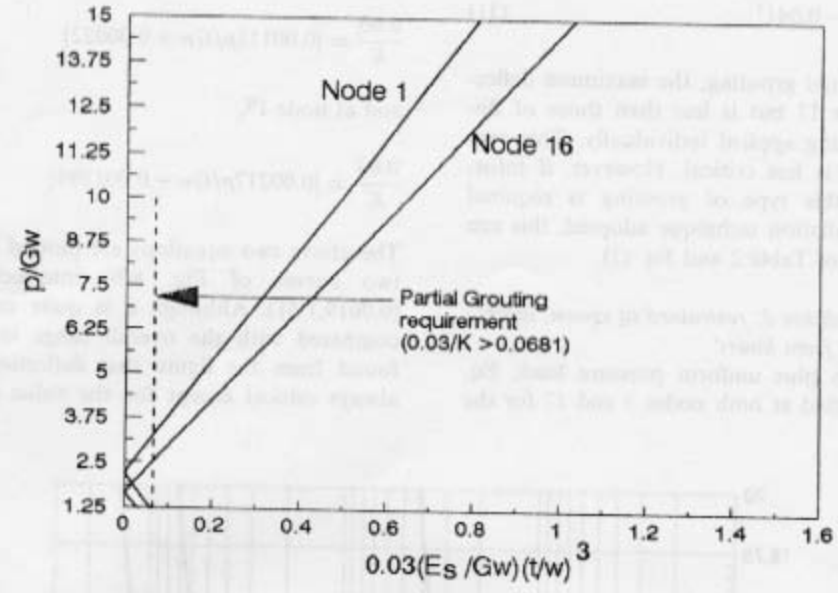

(a)

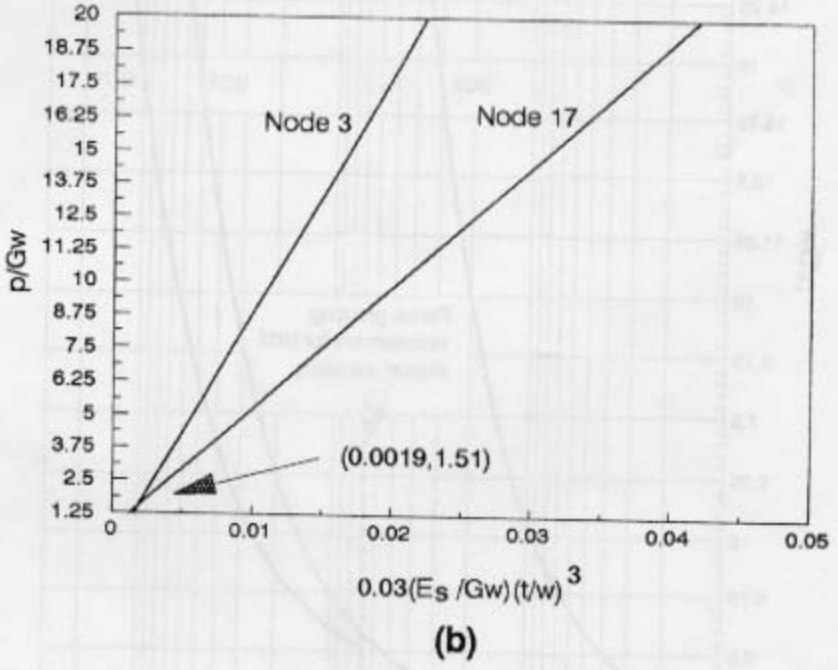

(b)

Fig. 8. Semielliptical-shaped lining: maximum deflections for flotation and additional external pressure under (a) boundary condition 1 at nodes 1 and 16, and (b) under boundary condition 3 at nodes 3 and 17 of the lining.

greater than h; as a result, the following design equation can be written:

$$\frac{0.03}{K} = |0.038p/Gw - 0.041| \tag{31}$$

For the case of partial grouting, the maximum deflection occurs at node 17 but is less than those of flotation or full grouting applied individually. This case of partial grouting is less critical. However, if information regarding this type of grouting is required because of the installation technique adopted, this can be found by means of Table 2 and Eq. (2).

9.2.3. Boundary condition 3: restrained at crown, invert and one-third height from invert

For full flotation plus uniform pressure load, Eq. (13) should be satisfied at both nodes 3 and 17 for the reason described earlier in case of boundary condition 1. Hence the following two design expressions can be found (using Eq. (13)): At node 3,

$$\frac{0.03}{K} = |0.00111p/Gw + 0.00022| \tag{32}$$

and at node 17,

$$\frac{0.03}{K} = |0.00217p/Gw - 0.001394| \tag{33}$$

The above two equations are plotted in Fig. 8(b). The two curves of Fig. 8(b) intersect at the point (0.0019,1.51). Although it is quite unimportant when compared with the overall range in Fig. 8(b), it is found from the figure that deflection at node 17 is always critical except for the value of p/Gw ranging

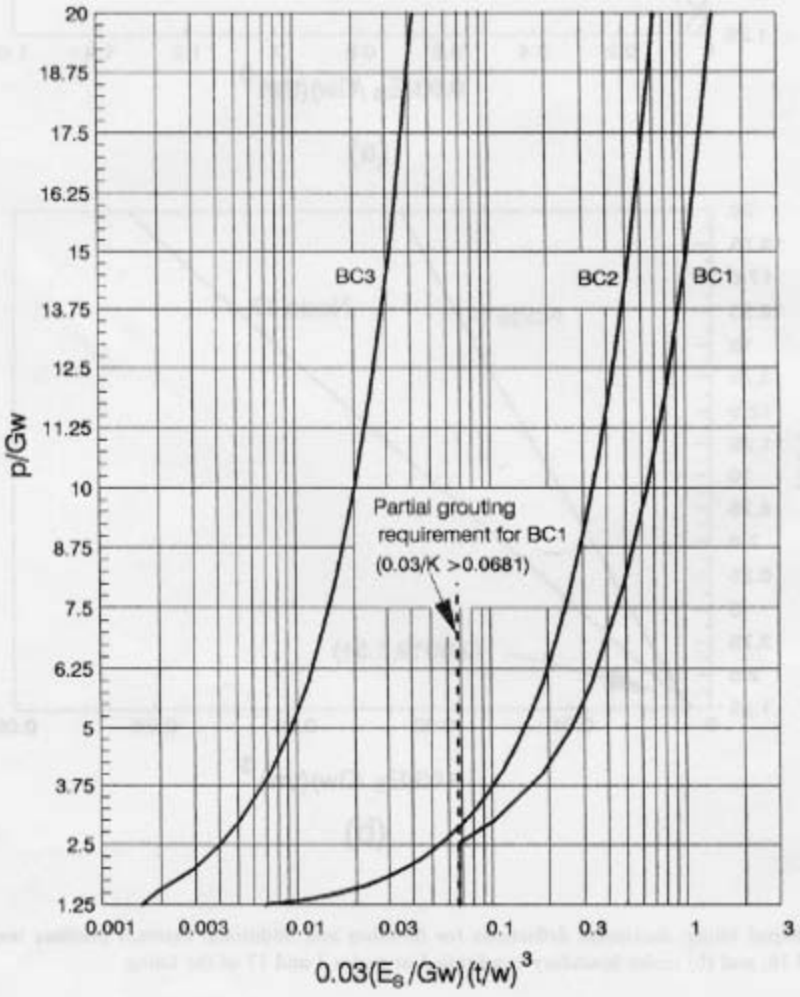

Fig. 9. Semielliptical-shaped lining: allowable grouting pressure based on deflection-limit criteria, for various boundary conditions.

from 1.25 to 1.51 within which the deflection at node 3 becomes slightly greater than that of node 17.

9.2.4. Summary of the deflection-limit criteria

Fig. 9 summarizes the results of the above three boundary conditions. This can now be used to determine the allowable grouting pressure on any particular lining, based on deflection-limit criteria. It can be seen in the figure that, unlike the cut-off of the curve for boundary condition 1 at an abscissa value of 0.0681, the curves for boundary conditions 2 and 3 gradually reach the horizontal axis.

Although, in the present study, the permissible deflection has been taken as 3% of the width of the sewer lining, the proposed design curves can be adopted without any modification for any other allowable deflection-limit criteria set by the competent authority. (Only the abscissa's label in Fig. 9 changes by replacing the factor 0.03 by $n/100$ where n is the permissible deflection as percentage of the width.)

9.3. Buckling criteria

9.3.1. Boundary condition 2: restrained at crown and invert

The dimensionless constants α and β for the maximum direct membrane stresses in the lining are listed in Table 3. For boundary condition 2, the maximum membrane stress develops at node 9 for both the cases of flotation load and uniform-pressure load. This leads to the following design expression. At node 9,

$$4Q(S_F/Gw) = 0.512 + 0.730(p/Gw - 1.25)$$
$$= 0.730p/Gw - 0.401 \quad (34)$$

9.3.2. Boundary condition 3: restrained at crown, invert and one-third height from invert

From Table 3, it can be seen that, under boundary condition 3, the maximum membrane stress develops at node 9 for the flotation load whereas, under uniform-pressure load, the maximum stress is located at node 21. Thus, Eq. (22) must be satisfied at both nodes 9 and 21. This leads to the following two design expressions. At node 9,

$$4Q(S_F/Gw) = 0.484 + 0.371(p/Gw - 1.25)$$
$$= 0.371p/Gw - 0.020 \quad (35)$$

At node 21,

$$4Q(S_F/Gw) = 0.212 + 0.504(p/Gw - 1.25)$$
$$= 0.504p/Gw - 0.418 \quad (36)$$

In order to visualize the effect of full-grouting load (i.e. combined flotation and uniform-pressure load), Eqs. (35) and (36) are plotted in Fig. 10. Evidently, Eq. (35) provides the design criterion up to a value of p/Gw equal to 2.993 (i.e. $4Q(S_F/Gw)$ equal to 1.090). Beyond this value, it is Eq. (36) which constitutes the design expression. (The combined membrane stresses

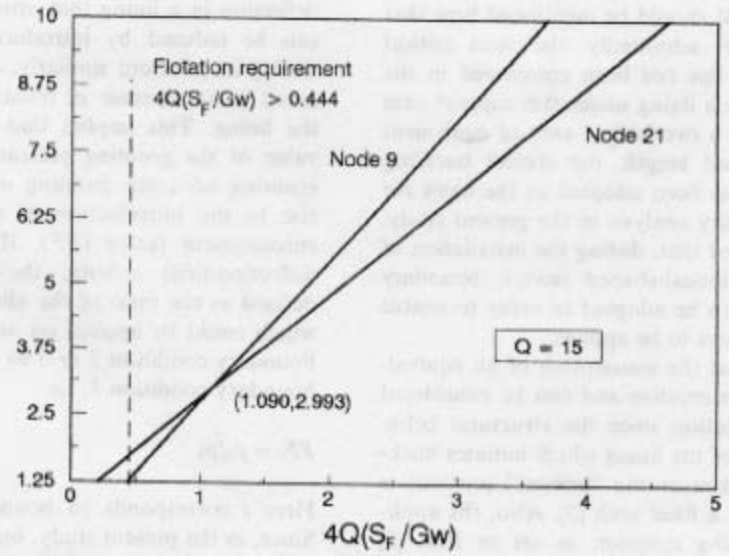

Fig. 10. Semielliptical-shaped lining: maximum membrane stresses at nodes 9 and 21 for flotation and additional external pressure under boundary condition 3.

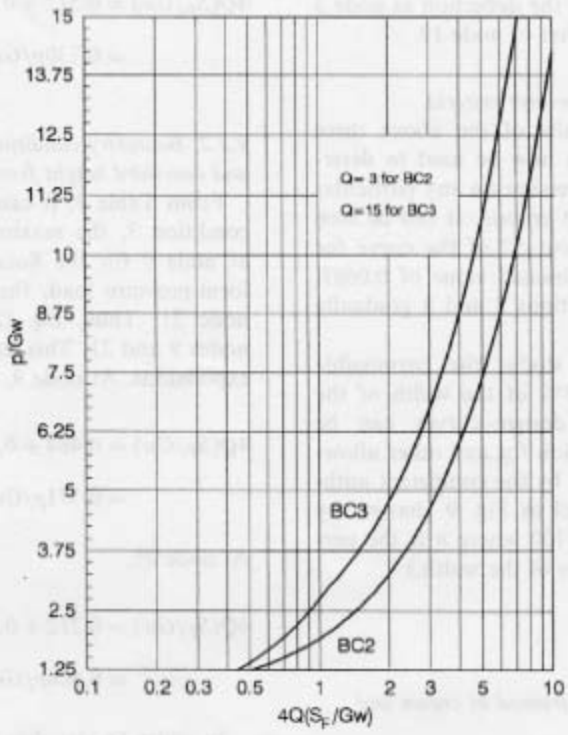

Fig. 11. Semielliptical-shaped lining: allowable grouting pressure, based on buckling criteria, for various boundary conditions.

at all other nodes were computed and were found to be less critical than those at nodes 9 and 21.)

9.3.3. Summary of the buckling criteria

Fig. 11 summarizes the results of the above two boundary conditions. It should be mentioned here that boundary condition 1—admittedly, the most critical buckling case of all—has not been considered in the buckling analysis since a lining under this support case cannot be idealized to a two-hinged arch of equivalent radius and unrestrained length, the critical buckling stress [10] of which has been adopted as the basis for the approximate stability analysis in the present study. Moreover, it is expected that, during the installation of linings within semielliptical-shaped sewers, boundary conditions 2 or 3 are to be adopted in order to enable higher grouting pressures to be applied.

It is to be noted that the assumption of an equivalent hinged arch is conservative and can be considered as a lower-bound solution since the structural behaviour of that portion of the lining which initiates buckling (and hence is taken as the "critical" portion) is between a hinged and a fixed arch [5]. Also, the applicability of the buckling criterion as set in Ref. [9] requires a uniform pressure intensity on the arch; such a condition may very nearly be fulfilled under excess head of grout.

10. Role of additional restraints during installation

10.1. Enhancement factor

Both the maximum bending stress and the maximum deflection in a lining that arise from grouting pressure can be reduced by introducing additional restraints during installation; similarly, additional restraints also result in an increase in resistance against buckling of the lining. This implies that an enhancement in the value of the grouting pressure can be achieved, thus ensuring adequate grouting of the annulus, and gives rise to the introduction of what can be termed an enhancement factor (EF). Here, for stress-limit and deflection-limit criteria, the enhancement factor is defined as the ratio of the allowable grouting pressure which could be applied on any particular lining using boundary condition 2 or 3 to the one corresponding to boundary condition 1, i.e.

$$EF_i = p_i/p_1 \tag{37}$$

Here i corresponds to boundary conditions 2 or 3. Since, in the present study, only boundary conditions 2 and 3 have been considered in the buckling analysis, the corresponding enhancement factor for this third criterion is given by p_3/p_2. In what follows, values of

EF are determined for each of the stress-limit, deflection-limit and buckling criteria. It has been observed that the *EF*s for deflection-limit criteria are much higher than their stress-limit and buckling counterparts, and, thus, will not govern the design. Again, under boundary condition 3, stress limitations of the material appear to always govern the design as well as the calculation of enhancement factors.

10.1.1. Stress-limit criteria

The expressions used to calculate the enhancement factors for stress-limit criteria can be derived from Eq. (23)–(28). Out of this group of equations, however, Eq. (25) does not govern beyond the flotation requirement (see Fig. 6b (node 26)); also, the range for which Eq. (27) (under BC3) is valid lies beyond the valid range of Eq. (23) and (24) (under BC1) so that Eq. (27) is also not involved in the final set of equations. Thus, although during the formulation of enhancement factors, Eqs. (25) and (27) have been considered, the ensuing final equations are not affected by them, but are governed by expressions (23), (24), (26) and (28) only. The final expressions are given below:

$$p_1 = 5.0(R + 0.042)Gw \quad \text{for } 0.428 \le R \le 0.844, \tag{38a}$$

$$= 2.5(R + 0.928)Gw \quad \text{for } R \ge 0.844, \tag{38b}$$

$$p_2 = 3.3(R + 0.277)Gw \quad \text{for } R \ge 0.197 \tag{39}$$

and

$$p_3 = 9.09(R + 0.0803)Gw \quad \text{for } R \ge 0.165 \tag{40}$$

Hence, the expression for enhancement factor can be written as follows:

$$(EF)_2 = 0.66\frac{R + 0.277}{R + 0.042} \quad \text{for } 0.428 \le R \le 0.844, \tag{41a}$$

$$= 1.32\frac{R + 0.277}{R + 0.928} \quad \text{for } R \ge 0.844 \tag{41b}$$

$$(EF)_3 = 1.818\frac{R + 0.0803}{R + 0.042} \quad \text{for } 0.428 \le R \le 0.844, \tag{42a}$$

$$= 3.636\frac{R + 0.0803}{R + 0.928} \quad \text{for } R \ge 0.844 \tag{42b}$$

The enhancement factors for boundary conditions 2 and 3, based on stress-limit criteria, are graphically shown in Fig. 12(a). It is seen from Fig. 12(a) that in the case of boundary condition 2, a value of R equal to at least 1.757 is needed in order to have an enhancement factor equal to or larger than 1. This means that no beneficial effect can be achieved by adopting boundary condition 2 if the value of R remains less than 1.757. Even then, the overall enhancement in the allowable grouting pressure due to the adoption of boundary condition 2 instead of boundary condition 1 during installation is not very significant. Adoption of boundary condition 3, on the other hand, always provides an enhancement factor greater than 1. Linings subjected to boundary condition 3 can readily bear about 2–3 times the grouting pressure sustainable by their boundary condition 2 counterparts.

10.1.2. Deflection-limit criteria

For deflection-limit criteria, the values of p_1, p_2 and p_3 are to be deduced from the set of Eqs. (29)–(33). However, in the calculation of *EF*s Eqs. (29) and (32) have not been found to be critical. It can be seen that Eq. (29) (node 1 in Fig. 8a) is not critical beyond the partial grouting requirement, while Eq. (32) (node 3 in Fig. 8b under BC3) is not important since the range in which it is valid is not covered by Eq. (30) (under BC1). The final expressions are given below:

$$p_1 = (0.03/K + 0.129)12.9Gw \quad \text{for } 0.03/K \ge 0.0681 \tag{43}$$

$$p_2 = (0.03/K + 0.041)26.32Gw \quad \text{for } 0.03/K \ge 0.0065 \tag{44}$$

$$p_3 = (0.03/K + 0.001394)460.83Gw \quad \text{for } 0.03/K \ge 0.0019 \tag{45}$$

From these expressions, enhancement factors for boundary conditions 2 and 3, based on deflection-limit criteria, can be derived as follows:

$$(EF)_2 = 2.04\frac{0.03/K + 0.041}{0.03/K + 0.129} \quad \text{for } 0.03/K \ge 0.0681 \tag{46}$$

$$(EF)_3 = 35.66\frac{0.03/K + 0.001394}{0.03/K + 0.129} \quad \text{for } 0.03/K \ge 0.0681 \tag{47}$$

Eqs. (46) and (47) are shown pictorially in Fig. 12(b). Similarly to the case based on stress-limit criteria, the adoption of boundary condition 2 during installation instead of boundary condition 1 hardly has any effect. Use of boundary condition 3, however, enhances the

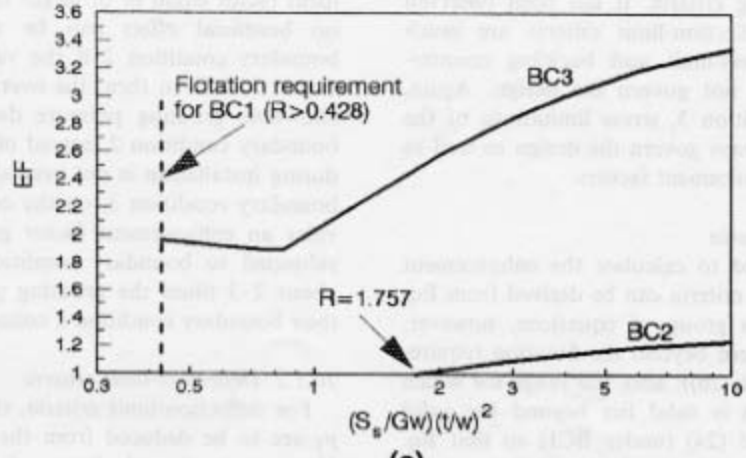

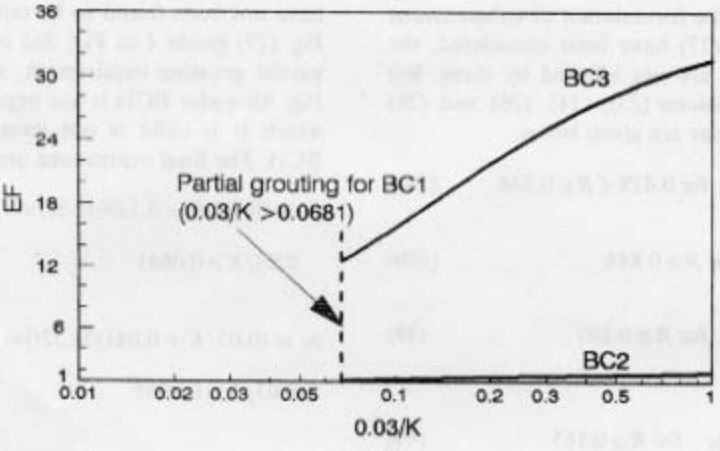

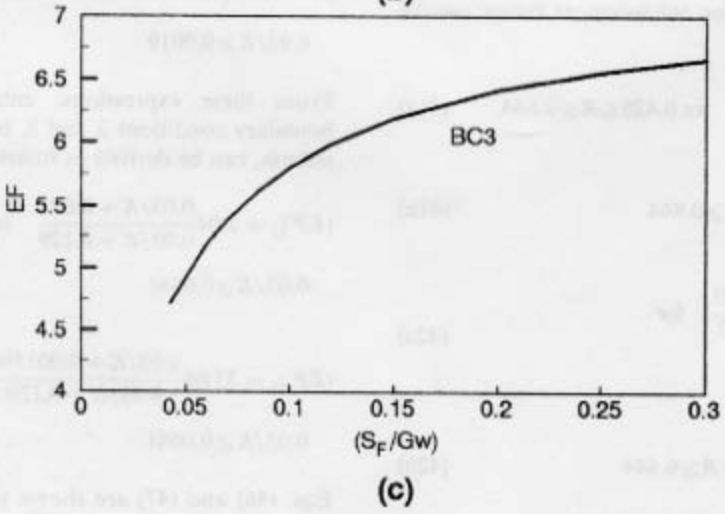

Fig. 12. Semielliptical-shaped lining: enhancement factors for allowable grouting pressure, based on (a) stress-limit criteria, (b) deflection-limit criteria, and (c) buckling criteria.

value of the allowable grouting pressure quite dramatically.

10.1.3. Buckling criteria

Through the use of Eqs. (34)–(36) the enhancement factor for the buckling criterion, due to the adoption of boundary condition 3 instead of boundary condition 2 during installation, can be found. In this exercise Eq. (35) (under BC3) has not been found to be relevant since it caters for a range of S_F/Gw for which no equation exists under BC2. The final expression is as follows:

$$EF_3 = p_3/p_2 = \frac{1.448(60S_F/Gw + 0.418)}{12S_F/Gw + 0.401} \quad \text{for} \quad S_F/Gw \geq 0.0426 \tag{48}$$

The enhancement factors corresponding to the buckling criterion are plotted in Fig. 12(c). It appears that linings subjected to the restraints of boundary condition 3 can sustain about 4–6 times the grout pressure allowable in the case of boundary condition 2.

10.2. Reduction factors

Once a value of allowable grouting pressure is determined for any particular lining using a certain restraint set-up, a considerable reduction in the allowable thickness of the lining can usually be achieved if additional restraints are used instead. This gives rise to the introduction of another factor, called the reduction factor (RF), which is defined below. It is clear from the findings of the previous section that, for a particular lining geometry and material properties, the enhancement factor achieved from stress-limit criteria is much lower than that based on deflection-limit criteria. Consequently, deflection-limit criteria do not govern the computation of enhancement factors. For this reason, the latter criteria have been excluded from the computation of reduction factors.

10.2.1. Stress-limit criteria

For such criteria, the reduction factor is defined as the ratio of the lining thickness resulting from the use of boundary condition 2 or 3 to the one corresponding to boundary condition 1. The equation used to calculate the values of RF is as follows:

$$RF_i = t_i/t_1 \tag{49a}$$

where

$$t_i = \left[C_i + (p/Gw - 0.8)E_i\right]^{1/2}\left[Gw^3/S_s\right]^{1/2} \tag{49b}$$

and

$$t_1 = \left[C_1 + (p/Gw - 0.8)E_1\right]^{1/2}\left[Gw^3/S_s\right]^{1/2} \tag{49c}$$

with i corresponding to boundary conditions 2 or 3, and other variables being defined by Eqs. (23)–(28) and Table 1. However, Eqs. (25) and (27) are not involved in the final expressions as Eq. (25) (node 26 in Fig. 6b) is not valid beyond the flotation requirement while the range of p/Gw for which Eq. (27) (under BC3) is valid is not catered for by Eqs. (23) and (24) (under BC1). The relevant equations that have been used to calculate the RFs are, then, as follows:

$$(RF)_2 = \left(\left|\frac{0.277 - 0.303p/Gw}{0.042 - 0.2p/Gw}\right|\right)^{1/2} \quad \text{for} \quad 2.35 \leq p \leq p/Gw \leq 4.43 \tag{50a}$$

$$= \left(\left|\frac{0.277 - 0.303p/Gw}{0.928 - 0.4p/Gw}\right|\right)^{1/2} \quad \text{for} \quad p \leq p/Gw \geq 4.43 \tag{50b}$$

$$(RF)_3 = \left(\left|\frac{-0.0803 + 0.11p/Gw}{0.042 - 0.2p/Gw}\right|\right)^{1/2} \quad \text{for} \quad 2.35 \leq p/Gw < 4.43 \tag{51a}$$

$$= \left(\left|\frac{-0.0803 + 0.11p/Gw}{0.928 - 0.4p/Gw}\right|\right)^{1/2} \quad \text{for} \quad p \leq p/Gw \geq 4.43 \tag{51b}$$

Here, similarly to the previous cases of EFs, the constraints of various RFs stem from the constraints of the equations on which they are dependent. Eqs. (50) and (51) are shown graphically in Fig. 13(a). It can be seen from the figure that considerably larger reduction factors are achieved by using boundary condition 3 when compared with boundary condition 2. Again, Fig. 13(a) shows that, for boundary condition 2, a minimum value of p_1/Gw equal to 6.7 is needed in order to achieve reduction factors less than one. Thus no beneficial effect can result from the use of boundary condition 2 if the value of p_1 is less than 6.7 Gw.

10.2.2. Buckling criteria

In the present study, the reduction factors corresponding to buckling criteria are given by the ratio t_3/t_2 since, as for the enhancement factors considered earlier, only boundary conditions 2 and 3 are considered. Using Eqs. (34), (35) and (36), the RF is found as follows:

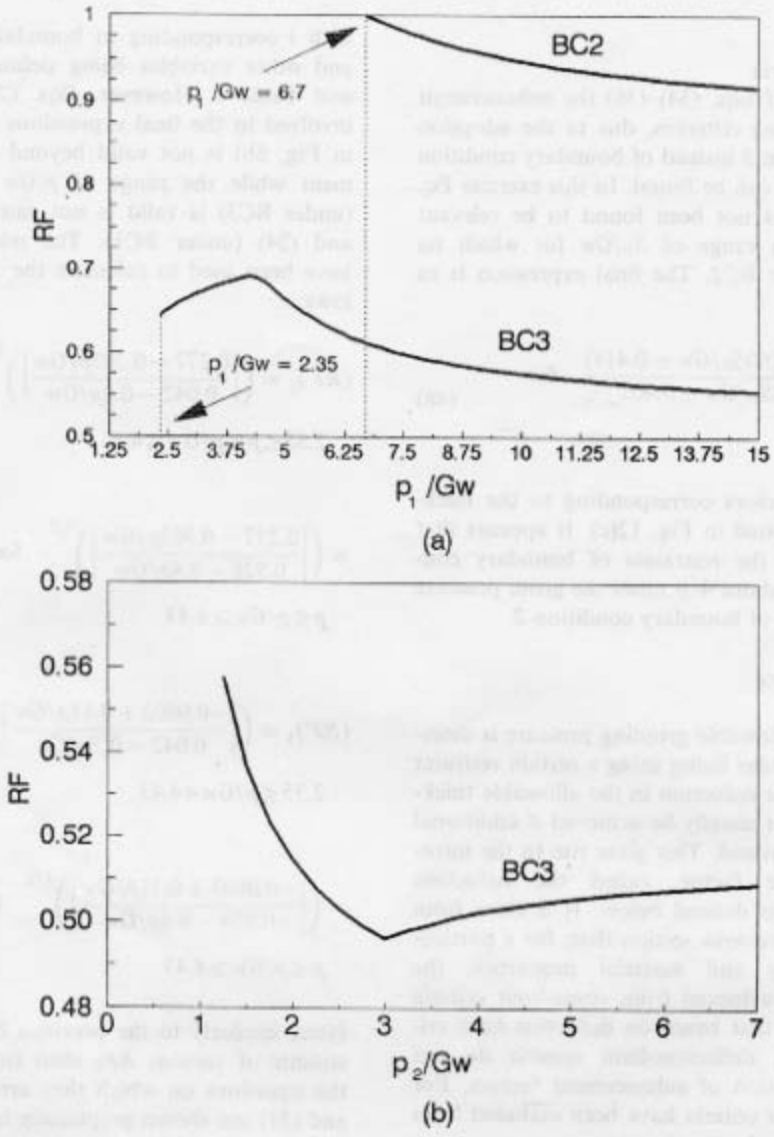

Fig. 13. Semielliptical-shaped lining: reduction factors for minimum permissible lining thickness based on (a) stress-limit criteria, and (b) buckling criteria.

$$RF_3 = t_3/t_2 = \left(\left|\frac{0.371p/Gw - 0.020}{5(0.730p/Gw - 0.401)}\right|\right)^{1/3} \quad \text{for } 1.25 \le p/Gw \le 2.993 \tag{52a}$$

$$= \left(\left|\frac{0.504p/Gw - 0.418}{5(0.730p/Gw - 0.401)}\right|\right)^{1/3} \quad \text{for } p/Gw \ge 2.993 \tag{52b}$$

The reduction factors based on the buckling criterion are shown in Fig. 13(b). The *RF*s for boundary conditions 2 and 3 were also determined on the basis of deflection-limit criteria. Again, stress and buckling limitations proved to be more critical for the determination of *RF*s, and hence reduction factors under deflection-limit criteria are not reported here. It appears that, whereas under boundary condition 2, either stress or buckling criteria may govern the determination of reduction factors, under boundary con-

dition 3, stress-limit criteria will invariably turn out to be the most critical consideration.

11. Conclusions

The proposed design curves can be used to determine the allowable grouting pressure during the installation of semielliptical-shaped sewer linings under various restraint set-ups and loading conditions. Alternatively, for a given boundary condition and known grouting pressure, the necessary lining thickness can be determined for any lining material using the currently proposed design curves and equations.

It has been shown that, by introducing additional temporary restraints before grouting around the semielliptical-shaped sewer lining, considerably higher grouting pressures, leading to a more reliable grouting operation, can usually be attained. Such enhancements in allowable grouting pressure are, however, more pronounced under the presently defined boundary condition 3 in comparison to its boundary condition 2 counterpart. In this study, it has been assumed that all restraints are fully effective, so that the restrained points of the lining are prevented from moving in any direction. Such ideal conditions will very nearly be realized if internal supports coupled with external packing are effectively provided.

In the case of the approximate buckling analysis, the introduction of additional restraints reduced the effective length of the arch between the restraints, thus leading to a stiffer structure with higher critical buckling pressure. The current buckling criterion assumes an uniform pressure intensity on the arch; the problem solved in Appendix A clearly shows that such a criterion may easily be achieved if linings of adequate thickness and acceptable physical properties are employed in the design; this is equivalent to the introduction of a minimum p/Gw value of, say, 3–4 (i.e. horizontal cut-offs at these values of the ordinate in Fig. 11), which implies that the head of grout is several times the size of the lining cross-section and thus means that the membrane stress state is nearly uniform.

Appendix A. Design example for a typical semielliptical-shaped lining

The following design example demonstrates the use of the structural design method outlined in the present paper. The use of a particular lining material is merely illustrative.

An existing sewer is of semielliptical shape. Its parameters are as follows:

1. Geometrical parameters. The overall height and width of the sewer are 1230 and 1000 mm, respectively. The minimum annulus grouting thickness to be provided is 25 mm, and the lining thickness t is 15 mm.
2. Material properties. The values of E_s, S_s and v of the GRP lining material are 20.0×10^6 kN/m^2, 60.0×10^3 kN/m^2 and 0.23, respectively. The G of the grout mix is 16.0 kN/m^3.

Using both boundary conditions 2 and 3 as the possible temporary support systems, the allowable grouting pressure is to be determined.

Solution

From the values of the geometrical parameters, the internal dimensions of the lining (h and w) are calculated as:

$$h = 1230 - (25 \times 2 + 15 \times 2) = 1150\ \text{mm}$$

$$w = 1000 - (25 \times 2 + 15 \times 2) = 920\ \text{mm}$$

Using the values of the material properties, the non-dimensional strength of the lining R, permissible deflection $0.03/K$ and non-dimensional stiffness of the lining S_F/Gw are calculated, enabling checks on the three criteria to proceed; these are as follows for boundary condition 2:

1. *(Bending) stress-limit criteria*—using the values of material properties, the non-dimensional strength R of the lining is calculated:

$$R = \left(\frac{S_s}{Gw}\right)\left(\frac{t}{w}\right)^2 = \frac{60 \times 10^3}{16.0 \times 0.92}\left(\frac{0.015}{0.92}\right)^2 = 1.084$$

   Using the value of R equal to 1.084 and Fig. 7 (or Eq. (26)), $p/Gw = 4.49$.
2. *Deflection-limit criteria*

$$\frac{0.03}{K} = 0.03\left(\frac{Es}{Gw}\right)\left(\frac{t}{w}\right)^3$$

$$= 0.03\left(\frac{20 \times 10^6}{16.0 \times 0.92}\right)\left(\frac{0.015}{0.92}\right)^3 = 0.1766$$

   Using the value of $0.03/K$ equal to 0.1766 and Fig. 9 (or Eq. (31)), $p/Gw = 5.73$.
3. *Buckling criteria*

$$S_F = \frac{1}{12}\frac{E_s}{1 - v^2}\left(\frac{t}{w}\right)^3 = \frac{1}{12}\left(\frac{20 \times 10^6}{1 - 0.23^2}\right)\left(\frac{0.015}{0.920}\right)^3$$

$$= 7.63$$

From this,

$$\frac{S_F}{Gw}4Q = \frac{7.63}{16 \times 0.92} \times 4 \times 3 = 6.22$$

Using this value and Fig. 11 (or Eq. (34)), $p/Gw = 9.07$.

Hence, the minimum of these three values, i.e. $p/Gw = 4.49$ (corresponding to the (bending) stress-limit criterion), is to be adopted as the basis for the design.

Here, $p/Gw = 4.49$, or $p = 4.49 \times 16.0 \times 0.92 = 66.09$ kN/m^2 which is equal to 4.13 m head of grout from the invert or 2.98 m head of grout from the crown of the lining.

When the above exercise is repeated for boundary condition 3, the values of p/Gw under stress-limit criteria, deflection-limit criteria and buckling criteria become 10.58, 82.02 and 62.53, respectively. Thus, under boundary condition 3, the value of p/Gw equal to 10.58 (corresponding again to the (bending) stress-limit criterion) governs, with allowable grouting pressure equal to 155.7 kN/m^2.

References

[1] Arnaout S, Pavlović MN. The structural behaviour of egg-shaped sewer linings with special emphasis on their current problems and research. In: Topping BHV, editor. Non-Conventional Structures Proceedings of the International Conference on the Design and Construction of Non-Conventional Structures, London, 8–10 December, vol. 2. Edinburgh: Civil–Comp Press, 1987. p. 231–8.

[2] Arnaout S, Pavlović MN. Studies on the structural behaviour of egg-shaped sewer linings under installation and operational conditions. Struct Engng Rev 1988;1:25–33.

[3] Arnaout S, Pavlović MN, Dougill JW. Structural behaviour of closely packed egg-shaped sewer linings during installation and under various restraint conditions. Proc ICE (Part 2) 1988;85:49–65.

[4] Pavlović MN, Arnaout S, Hitchins D. Finite element modelling of sewer linings. In: Topping BHV, editor. Developments in Structural Engineering Computing Proceedings of the Fifth International Conference on Civil and Structural Engineering Computing, Civil–Comp 93, Edinburgh, 17–19 August, vol. D. Edinburgh: Civil–Comp Press, 1993. p. 1–1.

[5] Pavlović MN, Arnaout S, Seraj SM. Some aspects of composite circular sewer linings under installation conditions. Engng Struct 1999;21:5–15.

[6] Seraj SM, Roy UK, Pavlović MN. Structural behaviour of closely packed inverted egg-shaped sewer linings during installation and under various restraint conditions. Thin-Walled Struct 1997;28:89–115.

[7] Seraj SM, Roy UK, Pavlović MN. Structural design of closely packed horseshoe-shaped sewer linings during installation. Thin-Walled Struct 1999;33:19–48.

[8] Sewerage Rehabilitation Manual. Swindon: Water Research Centre, 1983.

[9] Roy UK. Structural behaviour of closely packed sewer linings. MScEngg Thesis, Bangladesh University of Engineering and Technology, Dhaka, 1994.

[10] Timoshenko SP, Gere JM. Theory of Elastic Stability. New York: McGraw-Hill, 1961.